Available online at www.sciencedirect.com

SCIENCE DIRECT®

International Journal of Solids and Structures 42 (2005) 5536–5554

INTERNATIONAL JOURNAL OF SOLIDS and STRUCTURES

www.elsevier.com/locate/ijsolstr

# Seismic performance of multiple tuned mass dampers for soil–irregular building interaction systems ☆

Jer-Fu Wang [1], Chi-Chang Lin *

*Department of Civil Engineering, National Chung Hsing University, 250 Kuo-Kuang Road, Taichung, Taiwan 40227, ROC*

Received 18 February 2005
Available online 19 April 2005

**Abstract**

This paper deals with the applicability of multiple tuned mass dampers (MTMD) on the vibration control of irregular buildings modelled as torsionally coupled structures due to base motions considering the soil–structure interaction (SSI) effect. An efficient modal analysis methodology is used to systematically assess the combined soil–structure interaction and torsional coupling effects on asymmetric buildings. This method is implemented in the frequency domain to accurately incorporate the frequency-dependent foundation impedance functions. The performance index of MTMD is established based on the foundation-induced building floor motions with and without the installation of MTMDs. Unlike the traditional MTMD design criteria, the frequency ratio of each MTMD substructure to the controlled structural frequency is independent, in this paper, so that the MTMD with the optimal parameters can actually flatten the transfer functions of building responses. Numerical verifications show that the increase of height–base ratio of an irregular building and the decrease of relative stiffness of soil to structure generally amplify both SSI and MTMD detuning effect, especially for a building with highly torsionally coupled effect. With appropriately enlarging the frequency spacing of the optimal MTMDs, the detuning effect can be reduced. Moreover, the results of numerical investigations also show that the MTMD is more effective than single TMD as the SSI effect is significant.


*Keywords:* Multiple tuned mass dampers; Soil–structure interaction; Torsionally coupled building; Vibration control

☆ Contract/Grant sponsor: National Science Council, Republic of China; Contract/Grant name: NSC 89-2211-E-005-031.
* Corresponding author. Tel.: +886 4 22840438x225; fax: +886 4 22851992.
*E-mail addresses:* jerfu@ms16.hinet.net (J.-F. Wang), cclin3@dragon.nchu.edu.tw (C.-C. Lin).
[1] Tel.: +886 4 22862181.

0020-7683/$ - see front matter 
doi:10.1016/j.ijsolstr.2005.02.042

## 1. Introduction

Due to recent intensive analytical and experimental research, vibration control in structures using passive Tuned Mass Dampers (TMDs) is gaining more acceptance not only in the design of new structures and components but also in the retrofit of existing structures to enhance their reliability against winds, earthquakes and human activities (Lin et al., 2001). Since 1971, lots of TMDs have been successfully installed in high-rise buildings and towers. Most of these retrofits were reported to be effective in reducing structural dynamic responses.

Basically, a TMD is a device consisting of a mass connected to structures using a spring and a viscous damper. The TMD damping effect depends upon the fact that the TMD response delays the main structural response by a phase angle of 90°, so that the elastic force transmitted by the TMD acts like a viscous force on the main structure. This condition will not occur unless the TMD frequency is tuned to the frequency of the main structure and the excitation has this frequency content. Therefore, the structural property information is very essential for the optimum design of a passive TMD. In previous studies about TMDs, most of the researchers assumed that the controlled structural base is fixed, which is accurate only for structures built on rocks. In fact, many buildings are constructed on soft medium where the soil–structure interaction (SSI) effect may be significant. It is well known that the strong SSI effect would significantly modify the dynamic characteristics of structures such as natural frequencies, damping ratios and mode shapes (Veletsos, 1977; Wolf, 1985, 1988). Several researchers studied the SSI effect on the performance of TMD for planar buildings subjected to wind and earthquake excitations but led to different conclusions. Xu and Kwok (1992) investigated the wind-induced motion of two super tall structures (a 76-story RC building and a 370 m tower) mounted with TMD, taking into account the effect of soil compliancy under the footing. They claimed that soil compliancy will affect structural responses as well as the TMD effectiveness. Wu et al. (1999) focused on the TMD seismic performance for structures of shallow foundations. They performed numerical investigations for a specific TMD–structure (with height of 45 m) system built on soils with various shear wave velocities and found that the TMD effectiveness would decrease rapidly as the soil medium becomes softer. This is due to the fact that the entire soil–structure system gets more system damping for softer soil. The efforts of Gao et al. (1996) showed that the TMD is an effective vibration control device. However, the proposed elastic half-space model without considering material damping for soil which was not satisfied for seismic application was questionable and thought to be the reason that the TMD worked.

Since the SSI effect is generally difficult to be assessed accurately, the TMD detuning effect will occur because the TMD does not tune to the right frequency. To solve the problem, using MTMD is one of the promising solutions. The MTMD is a dynamic vibration control device that contains several parallel single-degree-of-freedom (SDOF) substructures. Each substructure has its own mass, damping ratio, and natural frequency. The MTMD systems with a uniform distribution of natural frequencies were first proposed by Xu and Igusa (1992) and then further investigated by many researchers (Yamaguchi and Harnpornchai, 1993; Abe and Fujino, 1994; Kareem and Kline, 1995; Jangid, 1995; Jangid and Datta, 1997; Li and Liu, 2003; Pansare and Jangid, 2003). It has been shown that the MTMD is more effective and reliable in the mitigation of structural vibration than single TMD (STMD). The original idea behind MTMD is to reduce the detuning effect through appropriately distributing the tuning frequencies, which is a critical and important issue to assure its vibration control effectiveness. The objective of this paper is then to investigate the influence of SSI effect on the performance of MTMD to suppress the excessive vibration of torsionally coupled buildings. An accurate approach to evaluate the soil–irregular building interaction effect in frequency domain developed by Wu et al. (2001) is employed to calculate the dynamic response for a building founded on soft soil under ground excitations. Two dimensionless parameters, stiffness ratio of soil relative to structure and slenderness ratio of structure, are introduced to fully examine the MTMD performance for various irregular buildings and soil conditions as SSI effect is significant. The optimization procedure to determine the system parameters (in particular the tuning frequencies) of an MTMD system considering torsionally coupled effect of the main structure is presented. To compare the vibration control effectiveness between MTMD and STMD, the response spectra for real earthquakes are also illustrated to ensure the benefit and reliability of MTMD.

## 2. System model and dynamic equations of motion

The system considered in this study, as shown in Fig. 1, is represented by a single-story building resting on the surface of a homogeneous elastic half-space. The structural model consists of a rigid floor of mass $m$, a rigid foundation of mass $m_b$, and axially inextensible columns of height $h$. The MTMD with $p$ numbers of parallel SDOF systems is installed on the floor moving in the $x$-direction. Each SDOF system contains a mass $m_{s_k}$ which connects with the floor by a damper $c_{s_k}$ and a spring $k_{s_k}$ and is located at a distance of $d_{s_k}$ from the $x$-axis, where $k = 1, 2, \ldots, p$. The floor level and the foundation mat are assumed to be of negligible thickness and of arbitrary shape. Two orthogonal principal axes of mass ($x$ and $y$) can be defined through the center of mass at the floor or at the foundation and the vertical axis of reference ($z$) passes through the center of mass. A uni-directional horizontal ground acceleration along the $x$-direction, $\ddot{x}_g$, is considered. For simplicity and without loss of generality, one way eccentricity between the centers of mass and resistance along the $y$-direction denoted by $e$ is considered in this study. Proportional viscous damping is assumed for the building such that the superstructure possesses classical normal modes. Complete binding is also assumed between the foundation and the supporting soil, which is characterized by its mass density, $\rho$, shear wave velocity, $v_s$, and Poisson's ratio, $\upsilon$.

The dynamic behavior of the investigated torsionally coupled building subject to a free-field ground motion $x_g$ can be completely described by the following five degrees of freedom: horizontal translation of the floor with respect to the foundation, $u$; twist about the $z$-axis of the floor with respect to the foundation, $\theta$; horizontal translation of the foundation, $x$; rocking about the $y$-axis of the whole building, $\phi$; and twist about the $z$-axis of the foundation, $\theta_b$. Moreover, the displacement of the $k$th DOF of MTMD with respect to the installation location is represented by $v_{s_k}$. Applying the substructure method conventionally adopted in the SSI analysis, the response of the building–MTMD subsystem can be solved by using the interaction forces including horizontal shear, $V$, overturning moment, $M$, and torque, $T$, developed at the foundation–soil interface to replace the soil subsystem.

Since the parameters of soil are generally difficult to be accurately estimated, it is not appropriate to design the MTMD for an uncertain SSI system. In this paper, the MTMD is treated as a control device to alter the characteristics of the superstructure system. The undamped equations of motion for the investigated building–MTMD superstructure system can be expressed as

$$m(\ddot{u} + \ddot{x} + h\ddot{\phi}) + k_u(u - e\theta) = \sum_{k=1}^{p}(c_{s_k}\dot{v}_{s_k} + k_{s_k}v_{s_k}) \tag{1a}$$

$$J(\ddot{\theta} + \ddot{\theta}_b) + k_\theta\theta - k_u e(u - e\theta) = \sum_{k=1}^{p}(c_{s_k}\dot{v}_{s_k} + k_{s_k}v_{s_k})e_{s_k} \tag{1b}$$

$$m_{s_k}[\ddot{x} + \ddot{u} + h\ddot{\phi} + \ddot{v}_{s_k} + e_{s_k}(\ddot{\theta}_b + \ddot{\theta})] + c_{s_k}\dot{v}_{s_k} + k_{s_k}v_{s_k} = 0 \quad (k = 1, 2, \ldots, p) \tag{1c}$$

where $k_u$ and $k_\theta$ are the lateral and torsional story stiffness; $J$ and $J_b$ are the mass polar moments of inertia about the $z$-axis of the floor and the foundation, respectively. Defining $J = mr^2$ where $r$ = radius of gyration of the floor; $\lambda_e = e/r$; $\lambda_{s_k} = d_{s_k}/r$; $\omega_u = \sqrt{k_u/m}$; $\omega_\theta = \sqrt{k_\theta/J}$; $\omega_{s_k} = \sqrt{k_{s_k}/m_{s_k}}$; $\xi_{s_k} = c_{s_k}/2\omega_{s_k}m_{s_k}$,

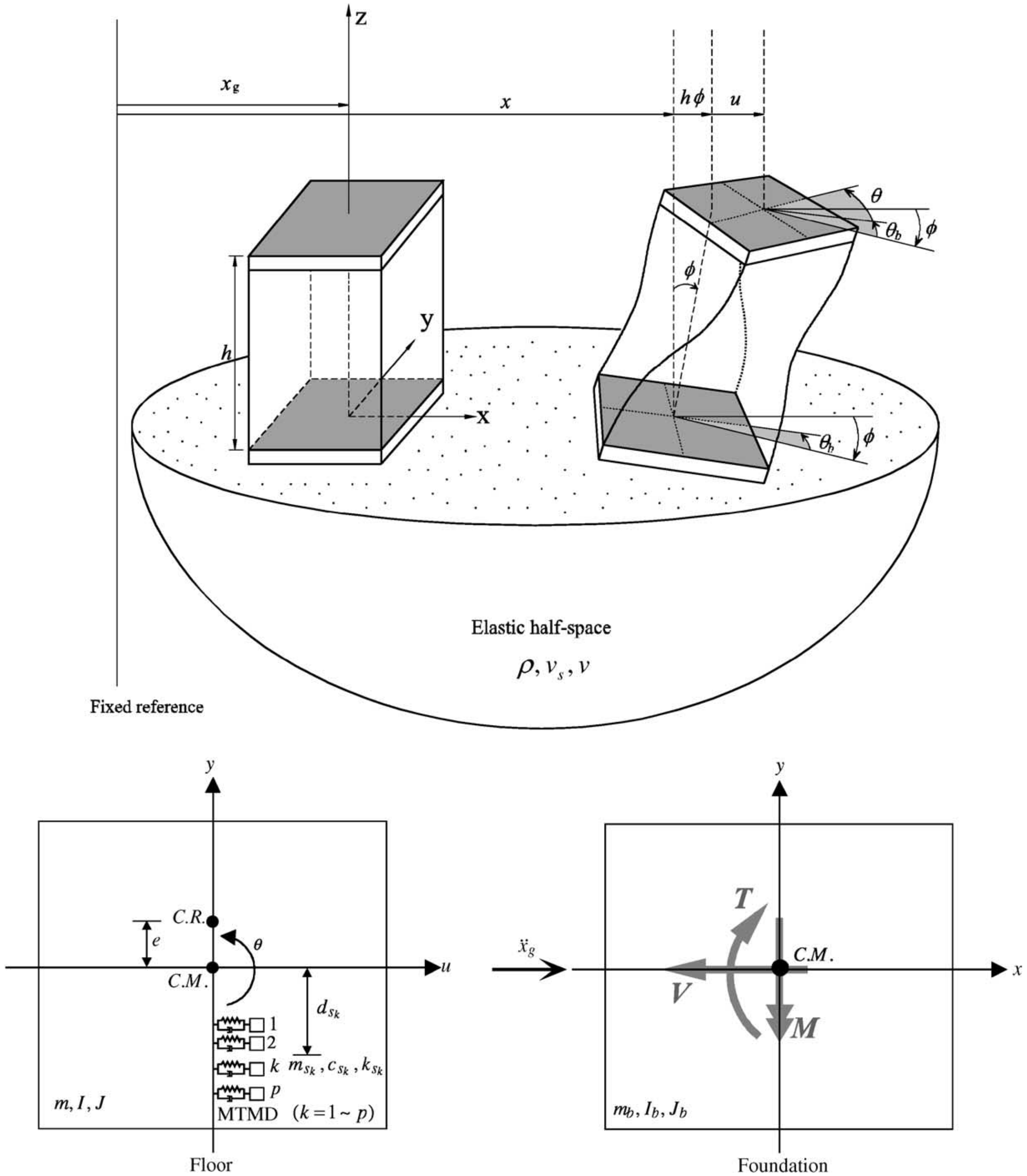


Fig. 1. Irregular building–MTMD–soil interaction model.

$\rho_{s_k} = m_{s_k}/m$, $u_\theta = r\theta$, $x_\phi = h\phi$ and $x_\theta = r\theta_b$, and applying structural damping, Eqs. (1a)–(1c) can be rearranged in matrix form as

$$\begin{bmatrix} \mathbf{M}_b & \mathbf{0} \\ \mathbf{M}_{sb} & \mathbf{M}_s \end{bmatrix} \begin{Bmatrix} \ddot{\mathbf{U}}_b \\ \ddot{\mathbf{U}}_s \end{Bmatrix} + \begin{bmatrix} \mathbf{C}_b & \mathbf{0} \\ \mathbf{0} & \mathbf{C}_s \end{bmatrix} \begin{Bmatrix} \dot{\mathbf{U}}_b \\ \dot{\mathbf{U}}_s \end{Bmatrix} + \begin{bmatrix} \mathbf{K}_b & \mathbf{0} \\ \mathbf{0} & \mathbf{K}_s \end{bmatrix} \begin{Bmatrix} \mathbf{U}_b \\ \mathbf{U}_s \end{Bmatrix} = \begin{Bmatrix} \mathbf{F}_b^{\mathrm{MTMD}} \\ \mathbf{0} \end{Bmatrix} + \begin{Bmatrix} -\mathbf{r}_b \\ -\mathbf{r}_s \end{Bmatrix} \ddot{\mathbf{X}}_b \tag{2}$$

where $\mathbf{M}_b$, $\mathbf{C}_b$, and $\mathbf{K}_b$ are $2 \times 2$ mass, damping, and stiffness matrices of building, and

$$\mathbf{M}_b = \begin{bmatrix} 1 & 0 \\ 0 & 1 \end{bmatrix}, \quad \mathbf{K}_b = \begin{bmatrix} \omega_u^2 & -\lambda_e \omega_u^2 \\ -\lambda_e \omega_u^2 & \omega_\theta^2 + \lambda_e^2 \omega_u^2 \end{bmatrix} \tag{3}$$

In Eq. (3), $\omega_u$ and $\omega_\theta$ represent the translational and torsional natural frequencies of the fixed-base torsionally uncoupled system, respectively. $\mathbf{M}_s$, $\mathbf{C}_s$ and $\mathbf{K}_s$ are $p \times p$ mass, damping and stiffness diagonal matrices of the MTMD system, respectively, and take the forms as

$$\mathbf{M}_s = I, \quad \mathbf{C}_s = \mathrm{diag}(2\xi_{s_k}\omega_{s_k}), \quad \mathbf{K}_s = \mathrm{diag}(\omega_{s_k}^2) \tag{4}$$

Moreover,

$$\mathbf{M}_{sb} = \begin{bmatrix} 1 & \lambda_{s_1} \\ 1 & \lambda_{s_2} \\ \vdots & \vdots \\ 1 & \lambda_{s_p} \end{bmatrix}, \quad \mathbf{r}_b = \begin{bmatrix} 1 & 1 & 0 \\ 0 & 0 & 1 \end{bmatrix}, \quad \mathbf{r}_s = \begin{bmatrix} 1 & 1 & \lambda_{s_1} \\ 1 & 1 & \lambda_{s_2} \\ \vdots & \vdots & \vdots \\ 1 & 1 & \lambda_{s_p} \end{bmatrix} \tag{5}$$

$\mathbf{U}_b^{\mathrm{T}} = \{ u \quad u_\theta \}$, $\mathbf{U}_s^{\mathrm{T}} = \{ v_{s_1} \quad v_{s_2} \quad \ldots \quad v_{s_p} \}$ and $\ddot{\mathbf{X}}_b^{\mathrm{T}} = \{ \ddot{x} \quad \ddot{x}_\phi \quad \ddot{x}_\theta \}$ are the building displacement vectors, MTMD stroke vector and the foundation excitation vector, respectively. Substituting

$$\mathbf{U}_b(t) = \mathbf{\Phi}\mathbf{q}(t) \tag{6}$$

into Eq. (2) where $\mathbf{\Phi} = \begin{bmatrix} \phi_{11} & \phi_{12} \\ \phi_{21} & \phi_{22} \end{bmatrix}$ is the $2 \times 2$ mode shape matrix of the fixed-base building and $\mathbf{q}(t)$ is the $2 \times 1$ modal displacement vector and multiplying $\mathbf{\Phi}^{\mathrm{T}}$ to the first row of Eq. (2), it becomes

$$\begin{bmatrix} \mathbf{M}_b^* & \mathbf{0} \\ \mathbf{M}_{sb}^* & \mathbf{M}_s \end{bmatrix} \begin{Bmatrix} \ddot{\mathbf{q}}(t) \\ \ddot{\mathbf{U}}_s(t) \end{Bmatrix} + \begin{bmatrix} \mathbf{C}_b^* & \mathbf{C}_{bs}^* \\ \mathbf{0} & \mathbf{C}_s \end{bmatrix} \begin{Bmatrix} \dot{\mathbf{q}}(t) \\ \dot{\mathbf{U}}_s(t) \end{Bmatrix} + \begin{bmatrix} \mathbf{K}_b^* & \mathbf{K}_{bs}^* \\ \mathbf{0} & \mathbf{K}_s \end{bmatrix} \begin{Bmatrix} \mathbf{q}(t) \\ \mathbf{U}_s(t) \end{Bmatrix} = \begin{Bmatrix} -\mathbf{\Gamma}_b \\ -\mathbf{r}_s \end{Bmatrix} \ddot{\mathbf{X}}_b(t) \tag{7}$$

where

$$(\mathbf{M}_{sb}^*)^{\mathrm{T}} = \begin{bmatrix} \phi_{11} + \phi_{21}\lambda_{s_1} & \phi_{11} + \phi_{21}\lambda_{s_2} & \cdots & \phi_{11} + \phi_{21}\lambda_{s_p} \\ \phi_{12} + \phi_{22}\lambda_{s_1} & \phi_{12} + \phi_{22}\lambda_{s_2} & \cdots & \phi_{12} + \phi_{22}\lambda_{s_p} \end{bmatrix}$$

$$\mathbf{C}_{bs}^* = \begin{bmatrix} -2\xi_{s_1}\omega_{s_1}\rho_{s_1}(\phi_{11} + \phi_{21}\lambda_{s_1}) & -2\xi_{s_2}\omega_{s_2}\rho_{s_2}(\phi_{11} + \phi_{21}\lambda_{s_2}) & \cdots & -2\xi_{s_p}\omega_{s_p}\rho_{s_p}(\phi_{11} + \phi_{21}\lambda_{s_p}) \\ -2\xi_{s_1}\omega_{s_1}\rho_{s_1}(\phi_{12} + \phi_{22}\lambda_{s_1}) & -2\xi_{s_2}\omega_{s_2}\rho_{s_2}(\phi_{12} + \phi_{22}\lambda_{s_2}) & \cdots & -2\xi_{s_p}\omega_{s_p}\rho_{s_p}(\phi_{12} + \phi_{22}\lambda_{s_p}) \end{bmatrix}$$

$$\mathbf{K}_{bs}^* = \begin{bmatrix} -\omega_{s_1}^2\rho_{s_1}(\phi_{11} + \phi_{21}\lambda_{s_1}) & -\omega_{s_2}^2\rho_{s_2}(\phi_{11} + \phi_{21}\lambda_{s_2}) & \cdots & -\omega_{s_p}^2\rho_{s_p}(\phi_{11} + \phi_{21}\lambda_{s_p}) \\ -\omega_{s_1}^2\rho_{s_1}(\phi_{12} + \phi_{22}\lambda_{s_1}) & -\omega_{s_2}^2\rho_{s_2}(\phi_{12} + \phi_{22}\lambda_{s_2}) & \cdots & -\omega_{s_p}^2\rho_{s_p}(\phi_{12} + \phi_{22}\lambda_{s_p}) \end{bmatrix}$$

$$\mathbf{\Gamma}_b = \begin{bmatrix} \phi_{11} & \phi_{11} & \phi_{21} \\ \phi_{12} & \phi_{12} & \phi_{22} \end{bmatrix}$$

Considering the orthogonality of $\mathbf{\Phi}$ and assuming proportional damping matrix, one can obtain $\mathbf{M}_b^* = \mathrm{diag} \cdot [\,1 \quad 1\,]$, $\mathbf{C}_b^* = \mathrm{diag} \cdot [\,2\xi_1\omega_1 \quad 2\xi_2\omega_2\,]$, $\mathbf{K}_b^* = \mathrm{diag} \cdot [\,\omega_1^2 \quad \omega_2^2\,]$ where $\xi_j$ and $\omega_j$ ($j = 1, 2$) are the $j$th modal damping ratio and modal frequency of the building.

## 3. Optimal design of MTMD

### 3.1. MTMD performance index

Taking the Fourier transformation for Eq. (7), the dynamic equations in frequency domain can be expressed as

$$\begin{aligned}\begin{Bmatrix}\mathbf{q}(\omega)\\ \mathbf{U}_s(\omega)\end{Bmatrix} &= \left(-\omega^2\begin{bmatrix}\mathbf{M}_\mathrm{b}^* & \mathbf{0}\\ \mathbf{M}_{s\mathrm{b}}^* & \mathbf{M}_s\end{bmatrix} + \mathrm{i}\omega\begin{bmatrix}\mathbf{C}_\mathrm{b}^* & \mathbf{C}_{\mathrm{b}s}^*\\ \mathbf{0} & \mathbf{C}_s\end{bmatrix} + \begin{bmatrix}\mathbf{K}_\mathrm{b}^* & \mathbf{K}_{\mathrm{b}s}^*\\ \mathbf{0} & \mathbf{K}_s\end{bmatrix}\right)^{-1}\begin{Bmatrix}-\boldsymbol{\Gamma}_\mathrm{b}\\ -\mathbf{r}_s\end{Bmatrix}\ddot{\mathbf{X}}_\mathrm{b}(\omega)\\ &= \begin{bmatrix}\mathbf{H}_\mathrm{bb}(\omega) & \mathbf{H}_{\mathrm{b}s}(\omega)\\ \mathbf{H}_{s\mathrm{b}}(\omega) & \mathbf{H}_{ss}(\omega)\end{bmatrix}\begin{Bmatrix}-\boldsymbol{\Gamma}_\mathrm{b}\\ -\mathbf{r}_s\end{Bmatrix}\ddot{\mathbf{X}}_\mathrm{b}(\omega)\end{aligned} \tag{8}$$

In the right-hand side of Eq. (8), the first matrix can be represented in detail as

$$\left[\begin{array}{cc|cccc} B_1' & 0 & C_1' & C_2' & \dots & C_p'\\ 0 & B_2' & E_1' & E_2' & \dots & E_p'\\ \hline D_1' & F_1 & G_1' & 0 & \dots & 0\\ D_2' & F_2' & 0 & G_2' & \dots & 0\\ \vdots & \vdots & \vdots & \vdots & \ddots & \vdots\\ D_p' & F_p' & 0 & 0 & \dots & G_p'\end{array}\right]^{-1} = \frac{1}{\omega_1^2 Q}\left[\begin{array}{cc|cccc} H_{11} & H_{12} & I_1 & I_2 & \dots & I_p\\ H_{21} & H_{22} & K_1 & K_2 & \dots & K_p\\ \hline J_1 & L_1 & M_{11} & M_{12} & \dots & M_{1p}\\ J_2 & L_2 & M_{21} & M_{22} & \dots & M_{2p}\\ \vdots & \vdots & \vdots & \vdots & \ddots & \vdots\\ J_p & L_p & M_{p1} & M_{p2} & \dots & M_{pp}\end{array}\right] \tag{9}$$

in which

$$B_j' = -\omega^2 + \mathrm{i}\omega(2\xi_j\omega_j) + \omega_j^2 = \omega_1^2[\beta^2 + \mathrm{i}(2\xi_j r_j) + r_j^2] = \omega_1^2 B_j$$

$$C_k' = \rho_{s_k,1}[-\mathrm{i}\omega(2\xi_{s_k}\omega_{s_k}) - \omega_{s_k}^2](\phi_{11} + \phi_{21}\lambda_{s_k}) = \omega_1^2\rho_{s_k,1}[-\mathrm{i}\beta(2\xi_{s_k}r_{f_k}) - r_{f_k}^2](\phi_{11} + \phi_{21}\lambda_{s_k}) = \omega_1^2 C_k$$

$$E_k' = \rho_{s_k,2}[-\mathrm{i}\omega(2\xi_{s_k}\omega_{s_k}) - \omega_{s_k}^2](\phi_{12} + \phi_{22}\lambda_{s_k}) = \omega_1^2\rho_{s_k,2}[-\mathrm{i}\beta(2\xi_{s_k}r_{f_k}) - r_{f_k}^2](\phi_{12} + \phi_{22}\lambda_{s_k}) = \omega_1^2 E_k$$

$$D_k' = -\omega^2(\phi_{11} + \phi_{21}\lambda_{s_k}) = \omega_1^2[-\beta^2(\phi_{11} + \phi_{21}\lambda_{s_k})] = \omega_1^2 D_k$$

$$F_k' = -\omega^2(\phi_{12} + \phi_{22}\lambda_{s_k}) = \omega_1^2[-\beta^2(\phi_{12} + \phi_{22}\lambda_{s_k})] = \omega_1^2 F_k$$

$$G_k' = -\omega^2 + \mathrm{i}\omega(2\xi_{s_k}\omega_{s_k}) + \omega_{s_k}^2 = \omega_1^2[-\beta^2 + \mathrm{i}\beta(2\xi_{s_k}r_{f_k}) + r_{f_k}^2] = \omega_1^2 G_k$$

where $j = 1, 2$ and $k = 1, 2, \ldots, p$. The elements of the first two rows of the matrix at right-hand side in Eq. (9) can be analytically solved and represented as

$$H_{11} = B_2 - \sum_{k=1}^{p}\frac{E_kF_k}{G_k}, \quad H_{12} = \sum_{k=1}^{p}\frac{C_kF_k}{G_k}$$

$$I_l = \frac{1}{G_l}\left(-B_2C_l + C_l\sum_{k=1(k\neq l)}^{p}\frac{E_kF_k}{G_k} - E_l\sum_{k=1(k\neq l)}^{p}\frac{C_kF_k}{G_k}\right)$$

$$H_{21} = \sum_{k=1}^{p}\frac{D_kE_k}{G_k}, \quad H_{22} = B_1 - \sum_{k=1}^{p}\frac{C_kD_k}{G_k} \tag{10}$$

$$K_l = \frac{1}{G_l}\left(-B_1E_l - C_l\sum_{k=1(k\neq l)}^{p}\frac{D_kE_k}{G_k} + E_l\sum_{k=1(k\neq l)}^{p}\frac{C_kD_k}{G_k}\right)$$

$$Q = \sum_{j=1}^{p-1}\sum_{k=j+1}^{p}\left(\frac{C_jD_jE_kF_k - C_jD_kE_kF_j - C_kD_jE_jF_k + C_kD_kE_jF_j}{G_jG_k}\right) - B_1\sum_{k=1}^{p}\frac{E_kF_k}{G_k} - B_2\sum_{k=1}^{p}\frac{C_kD_k}{G_k} + B_1B_2$$

From Eq. (8), the modal response vector of structure, $\mathbf{q}(\omega)$, can be extracted and takes the form as

$$\mathbf{q}(\omega) = -[\mathbf{H}_{\mathrm{bb}}(\omega)\boldsymbol{\Gamma}_{\mathrm{b}} + \mathbf{H}_{\mathrm{b}s}(\omega)\mathbf{r}_s]\ddot{\mathbf{X}}_{\mathrm{b}}(\omega) \tag{11}$$

or

$$\begin{Bmatrix} q_1(\omega) \\ q_2(\omega) \end{Bmatrix} = -\begin{bmatrix} H_{q_1\ddot{x}}(\omega) & H_{q_1\ddot{x}_\theta}(\omega) & H_{q_1\ddot{x}_\phi}(\omega) \\ H_{q_2\ddot{x}}(\omega) & H_{q_2\ddot{x}_\theta}(\omega) & H_{q_2\ddot{x}_\phi}(\omega) \end{bmatrix}\begin{Bmatrix} \ddot{X}(\omega) \\ \ddot{X}_\theta(\omega) \\ \ddot{X}_\phi(\omega) \end{Bmatrix} \tag{12}$$

where $H_{q_1\ddot{x}_i}(\omega)$ and $H_{q_2\ddot{x}_i}(\omega)$ are the transfer functions of $q_1(\omega)$ and $q_2(\omega)$ with respect to excitation $\ddot{X}_i(\omega)$, and

$$H_{q_1\ddot{x}_i}(\omega) = \sum_{k=1}^{2}H_{1k}\Gamma_{b,k1} + \sum_{k=1}^{p}I_k\Gamma_{s,k1} \tag{13}$$

$$H_{q_2\ddot{x}_i}(\omega) = \sum_{k=1}^{2}H_{2k}\Gamma_{b,k2} + \sum_{k=1}^{p}K_k\Gamma_{s,k2} \tag{14}$$

In Eq. (12), it is observed that the decrease of the amplitude of $H_{q_1\ddot{x}_i}(\omega)$ and $H_{q_2\ddot{x}_i}(\omega)$ indicates the reduction of structural modal responses. It is generally known that an earthquake excitation has wide-banded frequency content. Most of the dominant frequencies of building are smaller than the cutting-off frequency of the excitation spectrum. The mean-square response which is related to the area of the transfer function becomes important. Therefore, the MTMD performance index, $R_j$, is defined as

$$R_j = \frac{\int_0^\infty \left|H_{q_j\ddot{x}_i}(\omega)\right|^2_{\mathrm{MTMD}}\mathrm{d}\omega}{\int_0^\infty \left|H_{q_j\ddot{x}_i}(\omega)\right|^2_{\mathrm{NOMTMD}}\mathrm{d}\omega} \tag{15}$$

### 3.2. Optimization of MTMD parameters

In Eq. (15), the selection of $H_{q_j\ddot{x}_i}(\omega)$ is dependent upon the MTMD control goal. Moreover, $R_j$ is recognized as a function of structural parameters: $\xi_1$, $\xi_2$ and $\boldsymbol{\Phi}$, which should be known in prior, and the MTMD parameters: $\rho_{s_k}$, $\xi_{s_k}$, $r_{f_k}$ (the frequency ratio of the $k$th substructure to the controlled mode of the structure) and $\lambda_{s_k}$. The MTMD mass ratio is assigned based on construction costs and structural capacity considerations before the MTMD design. Moreover, assuming that each MTMD substructure has the same mass ratio and damping ratio $\xi_{s_0}$, and they are uniformly distributed at the central location ratio $\lambda_{s_0}$ with known spacing, the optimal MTMD parameters, $r_{f_1}, r_{f_2}, \ldots, r_{f_p}, \xi_{s_0}$ and $\lambda_{s_0}$ can be obtained through simultaneously solving the following equations:

$$\frac{\partial R_j}{\partial r_{f_1}} = \frac{\partial R_j}{\partial r_{f_2}} = \cdots = \frac{\partial R_j}{\partial r_{f_p}} = 0, \quad \frac{\partial R_j}{\partial \lambda_{s_0}} = 0, \quad \frac{\partial R_j}{\partial \xi_{s_0}} = 0 \tag{16}$$

### 3.3. Optimal location of MTMD

Theoretically, the MTMD optimal central location-ratio $(\lambda_{s_0})_{\text{opt}}$ is found from Eq. (16). However, in fact, the primary structural mode-shape functions contain some information for determining $(\lambda_{s_0})_{\text{opt}}$. From previous studies, it is well known that the optimal TMD location is at the position where the mode-shape value of the controlled mode is maximal. Moreover, as stated earlier, one set of MTMD is used for reducing one of the structural modes. As the high structural modes are significant, another set of MTMD must be installed. In this situation, the MTMD location should be carefully determined to avoid interaction among the MTMDs and unexpected amplification for the uncontrolled modes. From this point of view, the optimal MTMD location should satisfy the following both conditions as far as possible: (1) at the position where the mode-shape value of the controlled mode is maximum and (2) at the position where the mode-shape value of the uncontrolled mode is minimum. For the system model considered in this study, the optimal MTMD central location for controlling the first mode should satisfy the equation, $\phi_{12} + \lambda_{s_0}\phi_{22} = 0$, or

$$(\lambda_{s_0})_{\text{1st}} = -\frac{\phi_{12}}{\phi_{22}} \tag{17}$$

Similarly, the optimal MTMD central location-ratio for controlling the second mode then satisfies the equation, $\phi_{11} + \lambda_{s_0}\phi_{21} = 0$, or

$$(\lambda_{s_0})_{\text{2nd}} = -\frac{\phi_{11}}{\phi_{21}} \tag{18}$$

Fig. 2 illustrates the optimal MTMD locations for three cases of various $\lambda_e$ and $\lambda_\omega$. The dash-dot line represents the case of $\lambda_\omega(=\omega_\theta/\omega_u) \gg 1$, which the translational stiffness is weaker than the torsional stiffness so that the translational motion dominates the first mode. In this case, only one set of MTMD controlling the first mode is required. For various eccentricity ratio $\lambda_e$, it can be seen that the optimal location ratio $(\lambda_{s_0})_{\text{1st}}$ is close to zero. That indicates the optimum MTMD location is at the vicinity of the mass center of the floor. Since the torsional response is very small, the eccentrically installed MTMD to enhance the torsional resistance of the building is not required, as expected. However, when $\lambda_\omega \ll 1$, one set of MTMD controlling the torsional motion (the first mode) located at the vicinity of the positive floor edge is required. When $\lambda_\omega = 1$, translational and torsional modes are equally important. Two sets of MTMD located respectively near the vicinity of $\lambda_{s_0} = 1.0$ (which is at the opposite side of the center of floor rigidity) and $\lambda_{s_0} = -1.0$ (which is at the same side as the center of floor rigidity) are required.

### 3.4. Optimal mass–distribution ratio

For a highly torsionally coupled building, its dynamic responses are dominated by the first three modes. To reduce both the first and higher modal responses simultaneously, the MTMD mass should be divided into several appropriate parts to control all significant modes. The ratio of MTMD mass for higher mode to that for the first mode, which makes the structure response minimum, is called the optimal mass-distribution ratio. To illustrate this concept, the building model described in this study with a large eccentricity-ratio $\lambda_e = 0.3$, and two MTMDs systems with a total mass ratio of 2% are used as an example. The mean-square-response ratios $R_{u\ddot{x}}$ and $R_{u_\theta\ddot{x}}$ which are respectively defined as

$$R_{u\ddot{x}} = \frac{\int_0^\infty |H_{u\ddot{x}}(\omega)|^2_{\text{MTMD}}\,\mathrm{d}\omega}{\int_0^\infty |H_{u\ddot{x}}(\omega)|^2_{\text{NOMTMD}}\,\mathrm{d}\omega} \tag{19}$$

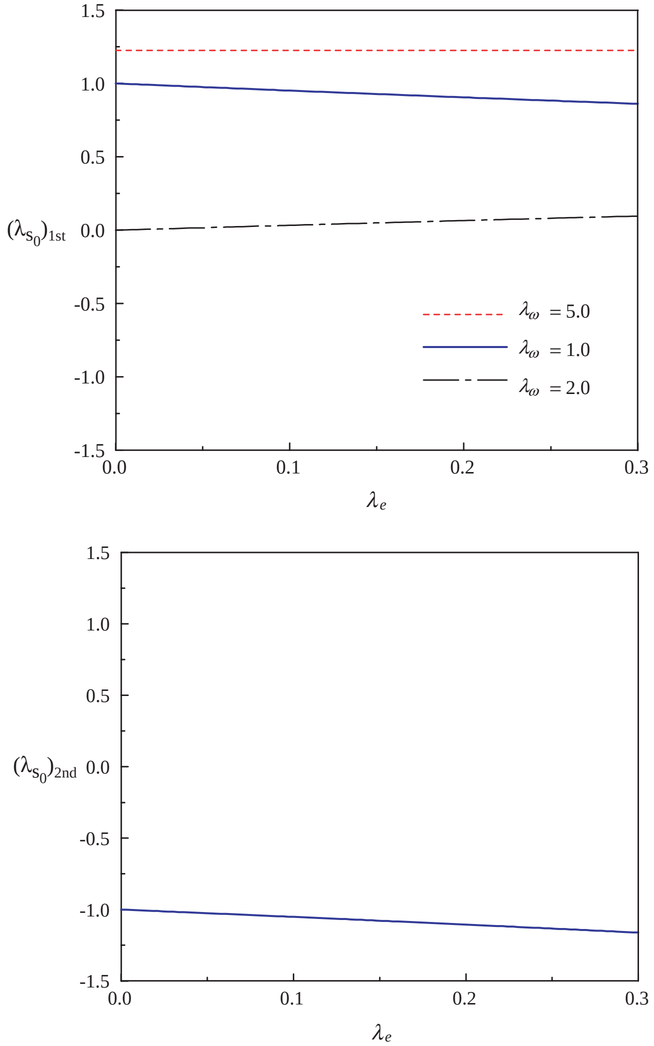


Fig. 2. Optimal MTMD planar location for an irregular building with various $\lambda_e$ and $\lambda_\omega$.

and

$$R_{u_\theta \ddot{x}} = \frac{\int_0^\infty \left|H_{u_\theta \ddot{x}}(\omega)\right|^2_{\mathrm{MTMD}} \mathrm{d}\omega}{\int_0^\infty \left|H_{u_\theta \ddot{x}}(\omega)\right|^2_{\mathrm{NOMTMD}} \mathrm{d}\omega} \tag{20}$$

are used to evaluate the MTMD control efficacy for translational and torsional responses, respectively. With the stiffness ratio $\lambda_\omega = 1.0$ and 2.0, the values of $R_{u\ddot{x}}$ and $R_{u_\theta \ddot{x}}$ with various mass-distribution ratio $\rho_{s,2}/\rho_{s,1}$ (where $\rho_{s,j}$ means the MTMD mass ratio for controlling the $j$th mode) are plotted in Fig. 3. It is found from the $R_{u\ddot{x}}$ curves that the optimal $\rho_{s,2}/\rho_{s,1}$ corresponding to the minimum value of $R_u\ddot{x}$ is zero for the case of $\lambda_\omega = 2.0$. That indicates it is beneficial to use the total MTMD mass to control the first modal response. This is reasonable because the building is rigid in torsional direction and the translational motion dominates the first modal response. Moreover, for the case of $\lambda_e = 0.3$ and $\lambda_\omega = 1.0$, both the first

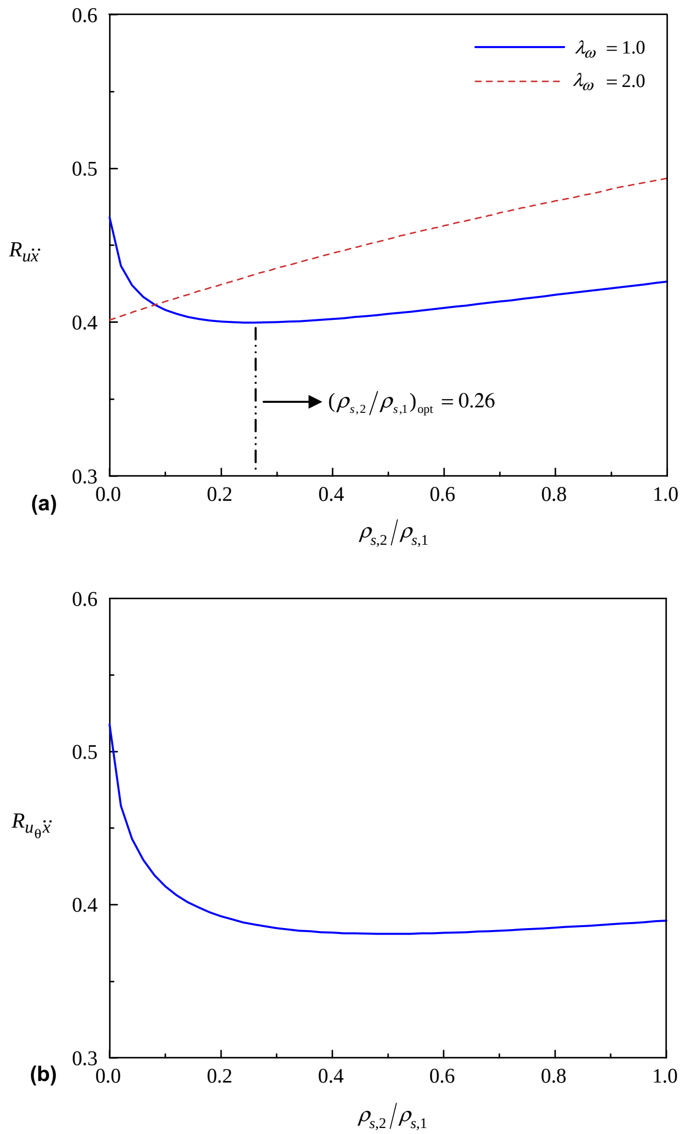


Fig. 3. Mean-square-response ratios $R_{u\ddot{x}}$ and $R_{u_\theta\ddot{x}}$ with different $\lambda_\omega$ for various MTMD mass-distribution ratios.

and second modes are important. Fig. 3(a) shows that the optimal $\rho_{s,2}/\rho_{s,1}$ which makes $R_{u\ddot{x}}$ minimum is about 0.26. From Fig. 3(b), we found that it also close to the optimal mass-distribution ratio for minimizing $R_{u_\theta\ddot{x}}$. It means the optimum MTMD mass ratios to control the first and second modal responses are 1.48% and 0.52%, respectively.

## 4. Numerical verifications

To verify the vibration control effectiveness of MTMDs, the transfer functions and the time-history responses of irregular buildings with and without MTMDs under real earthquake excitations are compared in this section. Three MTMD systems with same total mass but different number of substructures (for example, with 1, 3 and 7 substructures labeled as 'STMD', 'MTMD(3)' and 'MTMD(7)', respectively) are used to examine the influence of substructure number of MTMD systems on the vibration control effectiveness.

Table 1
Optimal MTMD parameters for cases 1–3 irregular building–MTMD systems

| Total mass ratio, $\rho_s$ | Building parameters | Controlled mode (mass ratio) | Number of substructures, $p$ | Location ratio, $\lambda_{s_k}$ | Damping ratio, $\xi_{s_0}$ | Frequency ratio, $r_{f_k}$ |
|---|---|---|---|---|---|---|
| 2% | Case 1: $\lambda_e = 0.3$, $\lambda_\omega = 2.0$ | First mode (2%) | 1 | 0.0962 | 7.0% | 0.968 |
| | | | 3 | 0.0462 | 3.3% | 0.902 |
| | | | | 0.0962 | | 0.968 |
| | | | | 0.1462 | | 1.044 |
| | | | 7 | −0.0538 | 1.8% | 0.871 |
| | | | | −0.0038 | | 0.905 |
| | | | | 0.0462 | | 0.936 |
| | | | | 0.0962 | | 0.967 |
| | | | | 0.1462 | | 1.000 |
| | | | | 0.1962 | | 1.037 |
| | | | | 0.2462 | | 1.083 |
| | Case 2: $\lambda_e = 0.3$, $\lambda_\omega = 1.0$ | First mode (2%) | 1 | 0.8612 | 9.2% | 0.948 |
| | | | 3 | 0.8112 | 4.4% | 0.864 |
| | | | | 0.8612 | | 0.946 |
| | | | | 0.9112 | | 1.046 |
| | | | 7 | 0.7112 | 2.5% | 0.826 |
| | | | | 0.7612 | | 0.864 |
| | | | | 0.8112 | | 0.901 |
| | | | | 0.8612 | | 0.939 |
| | | | | 0.9112 | | 0.982 |
| | | | | 0.9612 | | 1.032 |
| | | | | 1.0112 | | 1.098 |
| | Case 3: $\lambda_e = 0.3$, $\lambda_\omega = 1.0$ | First mode (1.59%) | 1 | 0.8612 | 8.2% | 0.958 |
| | | | 7 | 0.7112 | 2.2% | 0.846 |
| | | | | 0.7612 | | 0.881 |
| | | | | 0.8112 | | 0.915 |
| | | | | 0.8612 | | 0.950 |
| | | | | 0.9112 | | 0.988 |
| | | | | 0.9612 | | 1.033 |
| | | | | 1.0112 | | 1.091 |
| | | Second mode (0.41%) | 1 | −1.1612 | 4.9% | 1.324 |
| | | | 7 | −1.2062 | 1.2% | 1.230 |
| | | | | −1.1912 | | 1.266 |
| | | | | −1.1762 | | 1.297 |
| | | | | −1.1612 | | 1.328 |
| | | | | −1.1462 | | 1.359 |
| | | | | −1.1312 | | 1.393 |
| | | | | −1.1162 | | 1.435 |

Moreover, to illustrate the advantages of MTMD over TMD, their sensitivities of control performance on the estimation errors of primary structural parameters are investigated. Some practical considerations for the real implementation of MTMD system are also made.

### 4.1. Suppression of transfer function amplitude

To consider the torsion-coupling effect, three building–MTMD systems with same $\lambda_e = 0.3$ but different $\lambda_\omega$ are examined. Table 1 lists the optimal MTMD system parameters. Cases 1 and 2 are asymmetrical buildings with low and high coupling between the translational and torsional motions, respectively. The MTMDs for both buildings are designed to control the first modal responses. The case-3 building is same as that in case 2, but its MTMD is divided into two MTMD systems tuning to both the first and second modes. Fig. 4 shows the normalized transfer function amplitude of translation displacement (which is equal to the transfer function amplitude multiplying by $\omega_u$) with respect to the foundation translation for case-1 building with and without MTMDs. It is obvious to see that the first mode of building is separated into several small modes, where the number of peaks is equal to the number of MTMD substructure plus one. Moreover, the more number of substructures, the more reduction in both peak and mean-square responses for the building. Since the first mode dominates the entire structural response in case 1, the optimal MTMD mass distribution ratio for the second mode is zero. In other words, the MTMD is only used to control the first mode. It can also be seen that the local peaks of the transfer function with different MTMDs do not have the same magnitude. This is due to the fact that the MTMD optimization criteria is generated based on Eq. (16). Fig. 5 shows the normalized displacement transfer function for case-2 building with and without MTMDs. Because the torsional rigidity is small relative to translational rigidity and the eccentricity is large, the torsion-coupling effect becomes significant. The first and second modes are both important to the translational and torsional motions. Since the MTMD is only designed to control the first mode, it is thus seen that the second mode becomes more dominant after the installation of MTMDs. The transfer functions for case 3 are illustrated in Fig. 6. With the optimal MTMD mass distribution for two controlled modes, it is clearly seen that both the first and second modal amplitudes are significantly suppressed.

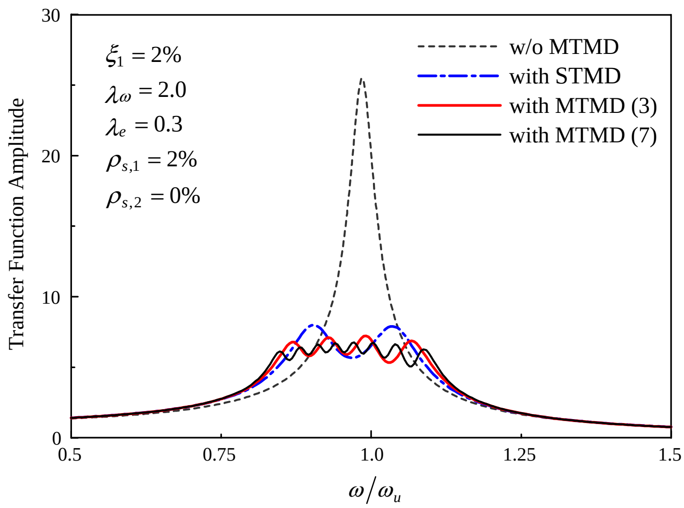


Fig. 4. Normalized transfer function of translation displacement for an irregular building with and without MTMDs controlling first mode.

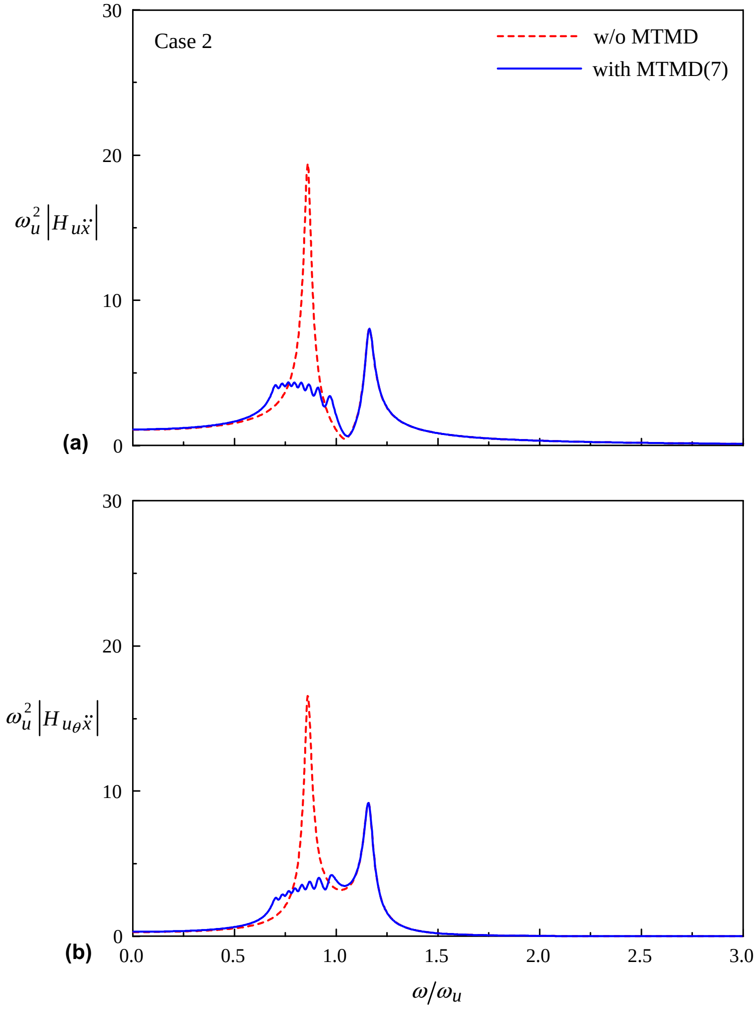


Fig. 5. Normalized transfer function amplitude of displacement for an irregular building with and without MTMDs controlling first mode.

### 4.2. Vibration control effectiveness of MTMD considering SSI effect

In this paper, the methodology developed by Wu et al. (2001) is employed to evaluate the floor response of irregular buildings with the consideration of SSI effect. The case-2 and -3 irregular building–MTMD systems mentioned in last section are investigated. Besides the system parameters shown in Table 1, other dimensionless SSI-related parameters of the torsionally coupled building-foundation–soil system used in this study are also listed in Table 2. For general buildings ($\lambda_h = h/r = 3$) and slender buildings ($\lambda_h = 5$), the mean-square-response ratios $R_{u\ddot{x}_g}$ under ground excitation $\ddot{x}_g$, are illustrated in Fig. 7 against $\sigma$ ranging from 0.5 to 5.0. Here, the parameter $\sigma$, is defined as $v_s/h\omega_u$ which is regarded as a measure of soil stiffness relative to the structure. Observe that when the soil is soft relative to the building (i.e., when $\sigma$ is small), STMD and MTMD become less effective. This results from the fact that the detuning effect occurs because the system properties change: the structural frequencies decrease and the damping ratio may increase or

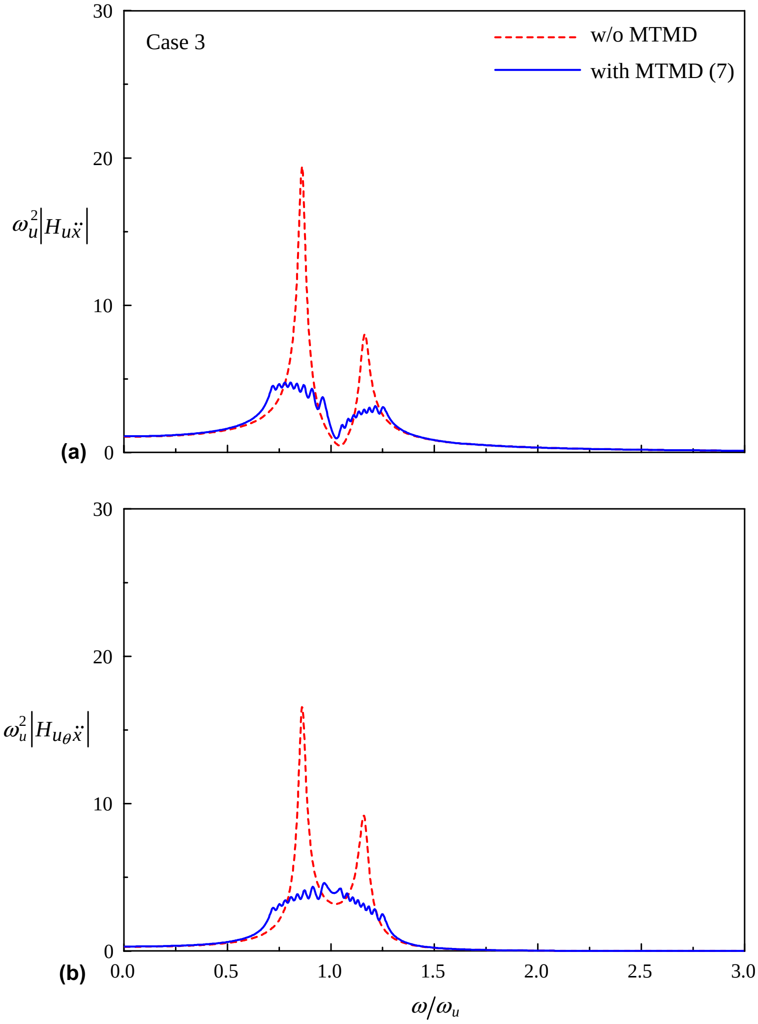


Fig. 6. Normalized transfer function amplitude of displacement for an irregular building with and without MTMDs controlling first two modes.

Table 2
Dimensionless SSI-related parameters for torsionally coupled building-foundation–soil system

| Category | Description | Notation | Magnitude |
|---|---|---|---|
| Structural parameters | Shape factor of structure | $\lambda_s = \frac{I}{J}$ | 0.5 |
| | Height-to-base ratio | $\lambda_h = \frac{h}{r}$ | 3.0, 5.0 |
| Foundation parameters | Mass ratio | $\delta_m = \frac{m_b}{m}$ | 0 |
| | Shape factor of foundation | $\delta_s = \frac{I_b}{J_b}$ | 0.5 |
| | Ratio of radius of gyration | $\delta_r = \frac{r_b}{r}$ | 1 |
| Soil parameters | Poisson's ratio | $v$ | 1/3 |
| | Relative stiffness of soil to structure | $\sigma = \frac{v_s}{h\omega_u}$ | 0.5–5.0 |
| | Relative density of structure to soil | $\gamma = \frac{m}{\rho r^2 h}$ | 0.5 |

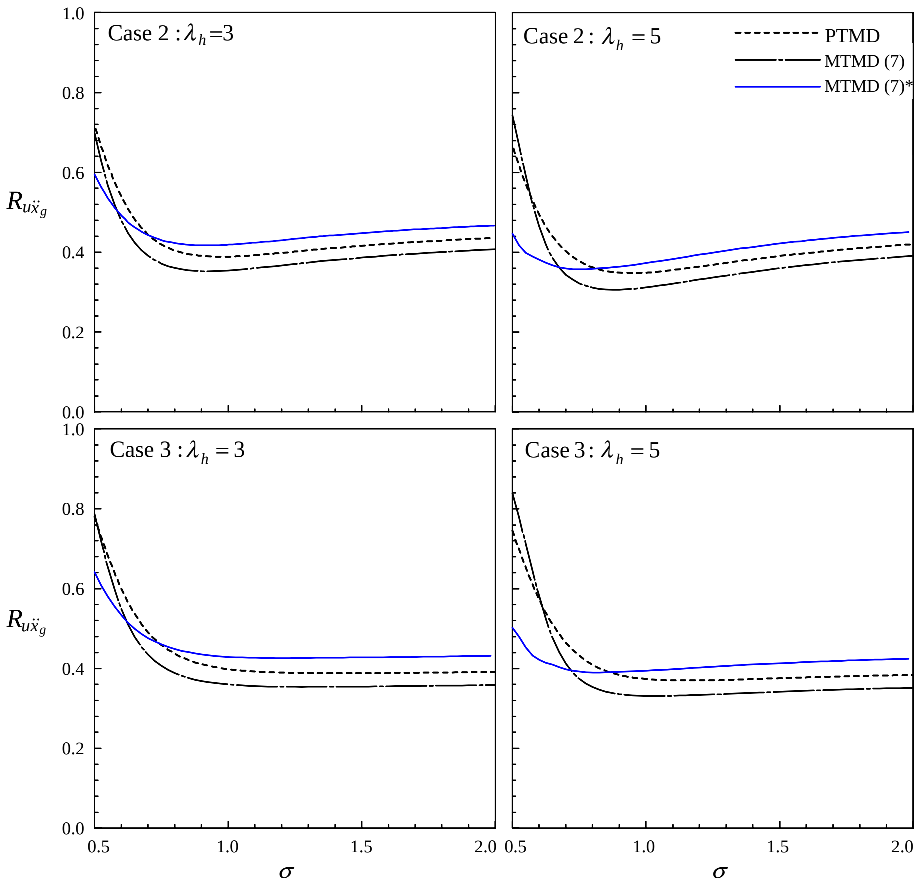


Fig. 7. Mean-square-response ratios of floor translation for an irregular building with STMD, MTMD(7) and MTMD(7)*.

decrease due to SSI effect. In most conditions, MTMDs have better control effectiveness than STMD except when $\sigma$ is less than about 0.75 and $\lambda_h = 5$. This phenomenon indicates that the sensitivity of MTMD to the variations in system parameters is higher than that of STMD. In order to improve the undesired MTMD detuning problem, MTMD with 100% enlarged frequency spacing is employed and the corresponding $R_{u\ddot{x}_g}$ is also shown in Fig. 7 (labeled as MTMD(7)*). It is seen that the improved MTMDs are less effective than optimal MTMDs when $\sigma$ is large, but indeed have better control effectiveness when the soil is very soft, in particular for buildings with large $\lambda_h$. The figure also shows that the case-3 MTMD has better performance than case-2 MTMD in most conditions as expected.

To evaluate the dynamic structural responses, the acceleration record (PGA = 0.821 g) of KJM000 component at the Japanese KJMA station during 1995 Kobe earthquake is used as the ground excitation. From Sikaroudi and Chandler (1992), it is known that for many practical types of building structure, $h\omega_u$ is approximately $60\pi$. Therefore, in this study the values $\sigma = 1.5$ corresponding to soft soil ($v_s \cong 280$ m/s) is used to represent the site conditions of the Kobe earthquake. The value $\sigma = \infty$ representing the fixed-base condition is also investigated to examine the influence of SSI effect. In order to consider the given irregular building with various $\omega_u(=2\pi/T_u)$ values, the corresponding $\lambda_h$ value should also be taken into account. In Sikaroudi and Chandler (1992), the empirical relationship between $\lambda_h$ and $T_u$ is approximately assumed to be $\lambda_h = 2T_u$. According to these conditions, the dynamic responses are calculated using the inverse Fourier

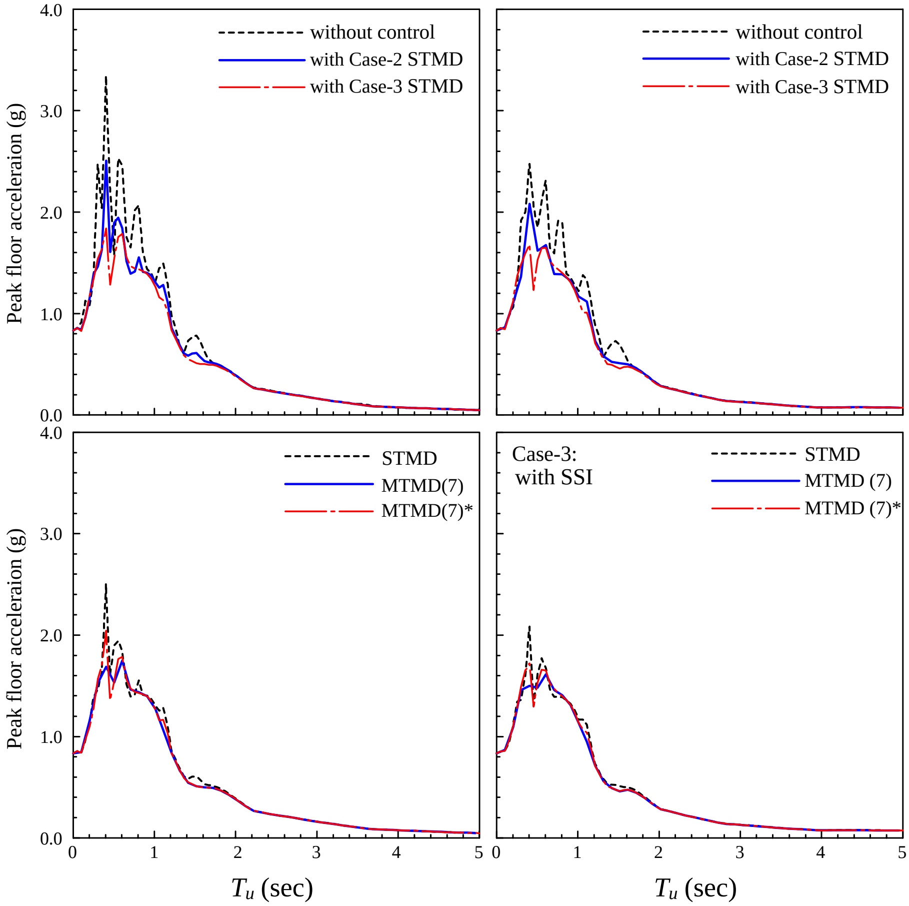


Fig. 8. Response spectra of floor translation of building–STMD and MTMD systems with and without considering SSI effect under the 1995 Kobe earthquake.

transform of the building response in frequency domain. Fig. 8 shows the peak floor translational acceleration of the irregular building with various values of $T_u$ under the Kobe earthquake. Comparing the curves with and without considering the SSI effect, it is found that the building response would generally be overestimated if the SSI effect is ignored. These figures also show that the STMD and MTMD control effectiveness is strongly dependent upon the frequency content of the earthquake. Moreover, the SSI effect decreases the STMD and MTMD effectiveness since the detuning effect occurs. If the SSI effect is not considered, the vibration control effectiveness will be overestimated. In addition, controlling two structural modes is the better strategy. The time history curves illustrated in Fig. 9 are the dynamic responses of floor translation for the building of $T_u = 0.4$ s in case 2 (or case 3) without and with various MTMDs considering SSI effect. It is clearly shown that not only the peak amplitude but the entire trace of the displacement and acceleration responses are significantly reduced due to the installation of MTMDs, in particular for the case-3 MTMD system in controlling two structural modes. Moreover, similar study is performed for buildings under an earthquake excitation measured at soft site. Fig. 10 shows the peak accelerations of floor translation for irregular buildings with various values of $T_u$ under the ground acceleration (PGA = 0.137 g) measured at TAP005 station in Taipei basin during the 1999 Taiwan Chi-Chi earthquake. It is obviously seen

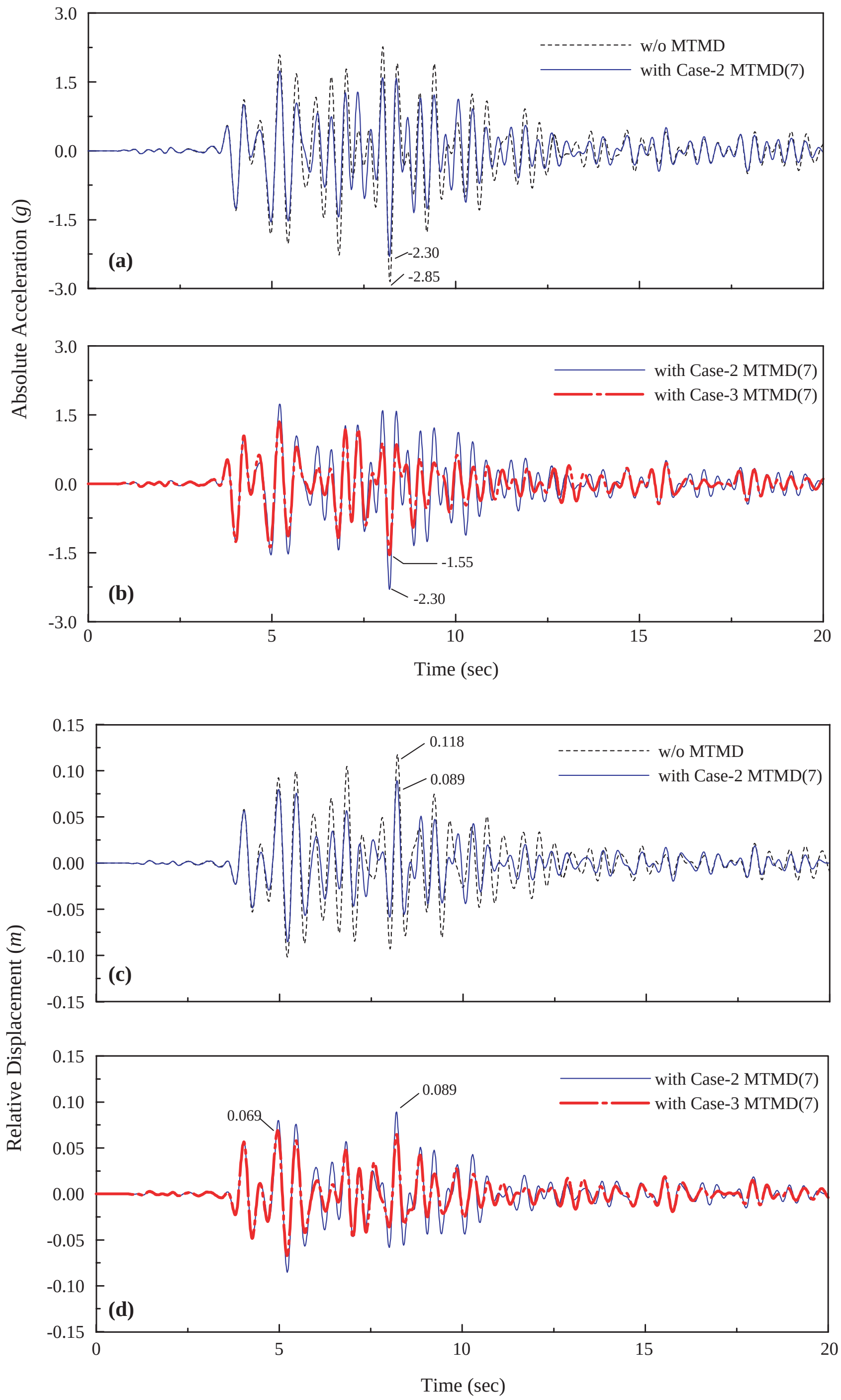


Fig. 9. Time histories of absolute acceleration and relative displacement of floor translation for case-2 and -3 building with and without various MTMDs considering SSI effect under the 1995 Kobe earthquake.

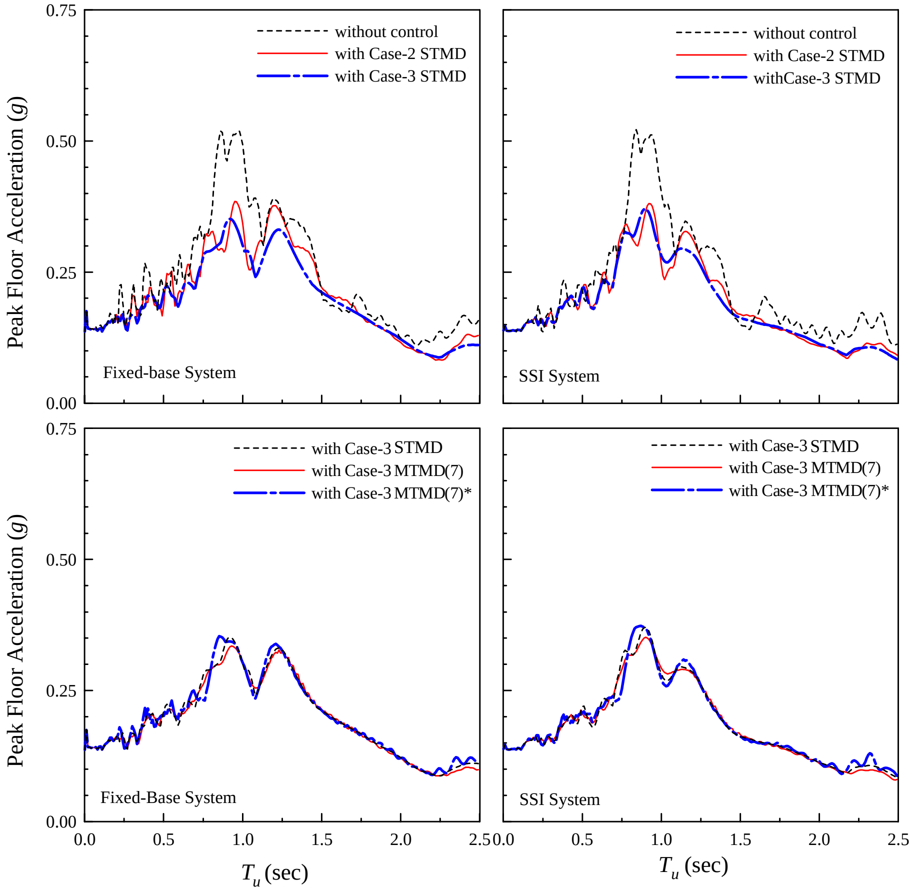


Fig. 10. Response spectra of floor translation of building–STMD and MTMD systems with and without considering SSI effect under the ground acceleration measured at Taipei Basin during the 1999 Taiwan Chi-Chi earthquake.

that the peak floor acceleration was reduced for the buildings with fundamental period close to that of the ground motion (about 0.8 s) due to the installation of STMD or MTMDs. Similar conclusions are drawn as those from Fig. 8.

## 5. Conclusions

The SSI effect indeed deteriorates the MTMD vibration control effectiveness. When an irregular building is built on soft soils, the SSI and torsionlly coupled effects should be considered to determine the optimal parameters of MTMD to avoid overestimating their effectiveness. Since a MTMD has many frequencies, its detuning effect can be reduced through appropriately adjusting the MTMD frequency spacing. It is the benefit which the STMD does not possess. The MTMD effectiveness is also dependent upon the characteristics of the external excitation. When the building dominant frequencies are located within the bandwidth of the external loading spectrum, MTMD can always reduce the building responses. It has been proven that the proposed MTMD is a useful vibration control device and more effective and robust than STMD.

## Acknowledgment

This study was supported by the National Science Council, Republic of China, under Grant NSC 89-2211-E-005-031. This support is greatly appreciated.

## References

Abe, M., Fujino, Y., 1994. Dynamic characterization of multiple tuned mass dampers and some design formulas. Earthquake Engineering and Structural Dynamics 23 (8), 813–835.

Gao, H., Samali, B., Kwok, K.C.S., 1996. Structural vibration control by passive dampers considering soil–structure interaction. In: Proceedings of 2nd International Workshop on Structural Control, HKUST, Hong Kong, pp. 174–185.

Jangid, R.S., 1995. Dynamic characteristics of structures with multiple tuned mass dampers. Structural Engineering and Mechanics 3 (5), 497–509.

Jangid, R.S., Datta, T.K., 1997. Performance of multiple tuned mass dampers for torsionally coupled system. Earthquake Engineering and Structural Dynamics 26, 307–317.

Kareem, A., Kline, S., 1995. Performance of multiple tuned mass dampers under random loading. Journal of Structural Engineering, ASCE 12 (2), 348–361.

Li, C., Liu, Y., 2003. Optimum multiple tuned mass dampers for structures under the ground acceleration based on the uniform distribution of system parameters. Earthquake Engineering and Structural Dynamics 32 (5), 671–690.

Lin, C.C., Wang, J.F., Ueng, J.M., 2001. Vibration control identification of seismically excited MDOF structure–PTMD systems. Journal of Sound and Vibration 240 (1), 87–115.

Pansare, A.P., Jangid, R.S., 2003. Tuned mass dampers for torsionally coupled systems. Wind and Structures 6, 23–40.

Sikaroudi, H., Chandler, A.M., 1992. Structure–foundation interaction in the earthquake response of torsionally asymmetric buildings. Soil Dynamics and Earthquake Engineering 11 (1), 1–16.

Veletsos, A.S., 1977. Dynamic behavior of building-foundation systems. In: Hall, W.J. (Ed.), Structural and Geotechnical Mechanics. Prentice-Hall, New Jersey, pp. 333–361.

Wolf, J.P., 1985. Dynamic Soil–structure Interaction. Prentice-Hall, New Jersey.

Wolf, J.P., 1988. Soil–structure Interaction Analysis in Time Domain. Prentice-Hall, New Jersey.

Wu, J.N., Chen, G.D., Lou, M.L., 1999. Seismic effectiveness of tuned mass dampers considering soil–structure interaction. Earthquake Engineering and Structural Dynamics 28 (11), 1219–1233.

Wu, W.H., Wang, J.F., Lin, C.C., 2001. Systematic assessment of irregular building–soil interaction using efficient modal analysis. Earthquake Engineering and Structural Dynamics 30 (4), 573–594.

Xu, K., Igusa, T., 1992. Dynamic characteristics of multiple substructures under closely spaced frequencies. Earthquake Engineering and Structural Dynamics 21, 1059–1070.

Xu, Y.L., Kwok, K.C.S., 1992. Wind induced response of soil–structure–damper systems. Journal of Wind Engineering and Industrial Aerodynamics 43 (3), 2057–2068.

Yamaguchi, H., Harnpornchai, N., 1993. Fundamental characteristics of multiple tuned mass dampers for suppressing harmonically forced oscillation. Earthquake Engineering and Structural Dynamics 22 (1), 51–62.